agronomy

MDPI

Article

A Spreading-Stem-Growth Mutation in *Lolium perenne*: A New Genetic Resource for Turf Phenotypes

Izolda Pašakinskienė [1,2,3]

[1] Botanical Garden, Vilnius University, Kairėnų 43, 10239 Vilnius, Lithuania; izolda.pasakinskiene@gf.vu.lt
[2] Life Sciences Center, Vilnius University, Saulėtekio 7, 10221 Vilnius, Lithuania
[3] Previous Institution: Institute of Agriculture, Lithuanian Research Centre for Agriculture and Forestry, Instituto al. 1, 58344 Akademija, Lithuania

Abstract

In *Lolium perenne*, a novel growth habit mutant, named *VIROIZ*, was recovered following colchicine treatment, and it was confirmed to maintain the diploid chromosome number ($2n = 2x = 14$). The mutation affected the stem morphology by inducing prolific axillary shoot formation at nodal zones, resulting in a spreading growth habit that can extend to ~70 cm in width. Inheritance analysis based on single-plant evaluations in crosses with wild-type plants (F_1, n = 285; F_2, n = 380) and in selfed progeny (S_1, n = 255) consistently showed ~40% expression of the spreading phenotype, deviating from classical Mendelian ratios and indicating complex genetic control. Phenotypic selection further distinguished divergent classes: positively selected lines ($C1^+$) averaged 3.90 axillary tillers per stem, whereas negatively selected lines ($C1^-$) averaged only 0.22. Partial sequencing of 11 candidate genes implicated in shoot architecture, covering 40–90% of full-length DNA, did not provide a conclusive explanation for the altered stem growth. Notably, a single point mutation was observed in *CRT3* (an endoplasmic reticulum chaperone that interacts with brassinosteroid signaling) highlighting it as a primary target for future studies. Cytological analysis of meiosis in F_1 hybrids between *VIROIZ* and wild-type plants revealed irregular chromosome pairing with persistent univalents (2–4 per cell), supporting the presence of structural chromosomal rearrangements that may disrupt gene organization and function in *VIROIZ*. The non-Mendelian segregation of the spreading phenotype, together with the observed meiotic irregularities, suggests that the mutation affects regulatory genes responsive to hormonal signals controlling axillary meristem initiation. The mutant represents a valuable resource for turf-type *L. perenne* breeding and for studying hormonal regulation of shoot morphogenesis in Poaceae.

Keywords: *Lolium perenne*; *VIROIZ* mutant; spreading growth habit; axillary shoot formation; stem branching; shoot morphogenesis; *CRT3*; brassinosteroid pathway; turfgrass breeding

Academic Editor: Chrysanthi Pankou

Received: 15 October 2025
Revised: 28 October 2025
Accepted: 29 October 2025
Published: 31 October 2025

Citation: Pašakinskienė, I. A Spreading-Stem-Growth Mutation in *Lolium perenne*: A New Genetic Resource for Turf Phenotypes. *Agronomy* **2025**, *15*, 2541. https://doi.org/10.3390/agronomy15112541

1. Introduction

Perennial ryegrass (*Lolium perenne* L.) is widely cultivated in temperate regions for both forage and turf due to its rapid growth, high nutritive value, good digestibility, and reliable seed production, making it one of the most prevalent species in temperate grasslands worldwide [1–7]. In turf applications, it is commonly included in mixtures for golf courses, sports fields, and lawns, where traits such as tiller density, ground coverage,

and persistence are emphasized over herbage yield [8,9]. Therefore, an intensive tillering habit that promotes dense, uniform turf is highly desirable in turf breeding.

Shoot development in perennial ryegrass has been described by Terrell [10] and Langer [11]. Each tiller consists of nodes bearing leaves and axillary meristems, most of which remain suppressed due to apical dominance, giving the species its typical bunch-type habit. Under specific conditions, however, axillary meristems can become active, producing secondary shoots, also referred to as stolons. Such creeping growth is rare in *L. perenne*, though sporadic occurrences have been reported in pastures [12–14]. More recently, distinct spreading forms have been described, including a patented stoloniferous subspecies *L. perenne* subsp. *stoloniferum* [15] and creeping cultivars used in turfgrass mixtures [9,16].

Shoot architecture is strongly regulated by hormonal networks. Auxins, cytokinins, and strigolactones interact to control apical dominance and the suppression of axillary meristems, thereby shaping shoot architecture [17–20]. Branching mutants have been reported in model and crop species, including *Arabidopsis thaliana* [21], pea [22], rice and wheat (review in [23]). However, to date, no naturally occurring or induced mutants affecting branching or tillering have been described in perennial ryegrass, despite its agronomic importance.

Here, we describe a novel spreading-growth mutant of *L. perenne*, designated *VIROIZ*, discovered among diploid plants treated with colchicine during an attempt to induce chromosome doubling [24]. While *L. perenne* is naturally diploid ($2n = 2x = 14$), colchicine is routinely used to generate tetraploids ($2n = 4x = 28$) for breeding [1]. In addition to inducing polyploidy, colchicine can cause heritable mutations affecting traits such as tillering, vegetative growth, and flowering [25]. *VIROIZ* was initially studied in the European GRASP project, which screened candidate genes in a set of 20 *L. perenne* genotypes [26]. This study identified variation in *LpBRI1*, a brassinosteroid receptor kinase gene, that suggested potential links to altered shoot morphology. More broadly, the brassinosteroid (BR) signaling pathway is well known for its central role in regulating shoot architecture, overall plant growth, and development [27,28].

To further investigate the genetic basis of *VIROIZ*'s unusual growth habit, we focused on eleven candidate genes with roles in hormone signalling and proteasome-mediated protein turnover. These include auxin- and brassinosteroid-related genes (*IAA1*, *BRI1*), strigolactone pathway regulators (*D27*, *CCD8*, *MAX2*), the brassinosteroid-associated chaperone *CRT3*, proteasome- and ubiquitin-related genes (*UBC4*, *UBC10*, *RHF2A*, *RPT2A*), and the protein kinase *CIPK9*.

Specifically, in this study, we (i) characterized the morphology of the mutant *VIROIZ* and the inheritance of the spreading growth type, (ii) assessed candidate genes (partial sequencing) and examined chromosome meiotic behavior aiming to explore potential changes linked to stem growth alteration in *VIROIZ* and (iii) evaluated *VIROIZ* potential as a genetic resource for turfgrass improvement and as a model for stem branching regulation.

2. Materials and Methods

2.1. Colchicine Treatment and VIROIZ Mutant Discovery

Seeds of diploid *L. perenne* representing a synthetic population were obtained from N. Lemežienė (Breeding Department, Lithuanian Institute of Agriculture). Embryos were excised from surface-sterilized seeds treated with a 0.3% (w/v) aqueous colchicine solution for 4 h and established in vitro on Murashige and Skoog (MS) medium [29] following the procedure described by [30]. A distinct mutant phenotype was identified among approximately 150 colchicine treated plants, each clonally propagated in duplicate. In field

evaluations, the mutant exhibited unique characteristics, including wide and bushy growth, as well as modifications in the inflorescence, reduced spikelet number and fasciation.

2.2. Plant Material and Field Evaluation of F_1, F_2, and S_1 Generations

To study the inheritance of the spreading-growth phenotype, five pairwise crosses were made between mutant and normal plants derived from the initial seed sample used for colchicine treatment. A total of 285 F_1 plants were grown at 50 × 50 cm spacing and evaluated for growth phenotype in the experimental field of the Lithuanian Institute of Agriculture (Figure S1). The F_2 generation was obtained through free crossing within five groups of F_1 plants, and 380 F_2 plants were evaluated under the same field conditions. The S_1 generations, S1-a and 1-b, were obtained by controlled self-pollination of cloned *VIROIZ* plants in two independent cycles, producing 113 and 142 plants, respectively. All trials were conducted under identical field conditions to ensure comparability. The soil at the experimental site was classified as Endocalcari–Epihypogleyic Cambisols (CMg-p-w-can) with pH 7.2, 159 mg kg^{-1} P_2O_5, 170 mg kg^{-1} K_2O, and 1.67% humus.

When the plants reached flowering, they were screened visually and classified into three categories based on their growth habit: mutant-type plants corresponding to *VIROIZ*, wild-type (WT) plants and intermediate-type plants that did not fully correspond to either phenotype. Intermediate plants did not attain the width of *VIROIZ* but were more widely spread than WT and displayed inflorescence abnormalities resembling those observed in *VIROIZ*. All assessments were performed by a single observer (I. Pašakinskienė) to ensure scoring consistency.

2.3. Divergent Selection for Axillary Tiller in the Greenhouse Pot Experiment

Five *L. perenne* genotypes (LTS03, LTS04, LTS11, LTS15, and LTS16) [31] were intercrossed in all possible pairwise combinations, including reciprocals, to form a synthetic C_0 population. Among them, LTS15 and LTS16 are ecotypes, LTS03 and LTS04 are parent genotypes of the VrA mapping population [32], and LTS11 is a mutant exhibiting enhanced axillary tillering [24]. Equal quantities of seed from each cross were sown individually in pots to establish 340 C_0 plants, which were evaluated for axillary tiller development by counting the mean number of axillary tillers per 20 primary tillers at the beginning of flowering. The 10% of plants with the highest and lowest mean axillary tiller numbers per stem in the plant (34 plants in each group) were selected to form subpopulations C_0S^+ and C_0S^-, respectively. These plants were intercrossed by open pollination in isolated greenhouses to produce $C_1{}^+$ and $C_1{}^-$ populations (Figure S1). To synchronize flowering, all plants were vernalized for 100 days at 6 °C under an 8 h photoperiod.

2.4. Candidate Gene Amplification, Sequencing, and Analysis

Candidate gene screening was performed at the Molecular Laboratory of the Botanical Garden, Vilnius University. Genomic DNA was extracted from fresh leaf tissue using the GeneJET Genomic DNA Purification Kit (Thermo Fisher Scientific, Vilnius, Lithuania) according to the manufacturer's instructions. Gene fragments of *IAA1* (*Indole-3-Acetic Acid inducible 1*), *BRI1* (*Brassinosteroid-Insensitive 1*), *D27* (*DWARF27*), *CCD8* (*Carotenoid Cleavage Dioxygenase 8*), *MAX2* (*More Axillary Growth 2*), *CRT3* (*Calreticulin 3*), *UBC4* (*Ubiquitin-Conjugating Enzyme 4*), *UBC10* (*Ubiquitin-Conjugating Enzyme 10*), *RHF2A* (*RING-H2 Finger Protein 2A*), *RPT2A* (*Regulatory Particle Triple-A ATPase 2A*), and *CIPK* (*CBL-Interacting Protein Kinase*) were amplified using original primers. The primers were designed with Primer3Plus (https://www.primer3plus.com) using *L. perenne* reference sequences from https://www.ncbi.nlm.nih.gov/nuccore/NC_067250.1/ (accessed on 14 October 2022). Primers for gene construction were designed to generate amplicons of approximately 800 bp, dividing the gene into smaller overlapping fragments. Each adjacent fragment

contained overlapping end regions to enable assembly. Primer melting temperatures (Tm) calculated using the Thermo Fisher Scientific "Tm Calculator." The primers were synthesized by METABION (Planegg, Germany).

PCR reactions (20 µL) contained 30 ng genomic DNA, 2.5 µM of each primer, 2.0 µM dNTP mix and 5 U/µL DreamTaq DNA Polymerase (Thermo Fisher Scientific, Vilnius, Lithuania), and 10x Polymerase buffer. The thermal cycling profile was: 95 °C for 2 s, followed by 35 cycles of 95 °C for 30 s, annealing temperature for 30 s, 72 °C for 60 s/kb. The reaction was terminated with extension at 72 °C for 5 min.

PCR products were visualized on agarose gels, excised and purified using the GeneJET Gel Extraction Kit (Thermo Fisher Scientific, Vilnius, Lithuania). The purified amplicons were sequenced in both directions by BaseClear B.V. (Leiden, The Netherlands) using the Sanger method. The high-quality sequences were assembled into contigs, aligned, and analyzed in AliView [33]. The sequence specificity was verified by BLAST (version BLAST+ 2.13.0) alignment against *L. perenne* reference genes. The reading frames and start codons were confirmed relative to reference sequences.

RNA was isolated from leaves using the GeneJET Plant RNA Purification Kit (Thermo Fisher Scientific, Vilnius, Lithuania) according to the manufacturer's instructions. cDNA synthesis was performed using the Maxima First Strand cDNA Synthesis Kit for RT-qPCR (Thermo Fisher Scientific, Vilnius, Lithuania) according to the manufacturer's instructions, with the incubation at 50 °C extended to 30 min.

2.5. Chromosome Pairing Analysis in Meiosis

For the analysis of chromosome pairing during meiosis, samples from *VIROIZ* and F_1 hybrids were collected at the young inflorescence stage and examined for the presence of meiotic metaphase I (MI). Samples were collected from 3 clonally propagated *VIROIZ* plants and from 10 F_1 hybrids at random. The young inflorescences were fixed in Carnoy's solution (ethanol:acetic acid, 3:1 *v*/*v*) and stored in 70% ethanol. Anthers were squashed in 1% acetocarmine, gently heated, and covered with a coverslip to spread meiocytes. The cells at Metaphase I were examined under a light microscope (1000× magnification), and the number of univalents, rod or ring bivalents, and multivalents was recorded in at least 50 cells.

2.6. Statistical Analysis

Phenotypic category frequencies were compared using chi-square tests. Sequence alignment statistics and variant calling were performed with AliView [33].

3. Results

3.1. VIROIZ Morphotype

Among the C_0 plants of *Lolium perenne* regenerated from isolated embryos treated with 0.3% aqueous colchicine, a unique mutant exhibiting an unusual growth habit was identified. Cytological analysis confirmed that the plant retained the diploid chromosome number ($2n = 2x = 14$). Morphologically, the mutant displayed a creeping, spreading growth pattern resulting from prolific axillary shoot formation, with additional shoots produced at each nodal zone (Figure 1A,B). The mutation also altered inflorescence morphology, leading to a reduced number of spikelets and the occurrence of fasciation symptoms (Figure 1C,D). This spreading growth mutant conferred vigorous growth, producing dense, prostrate, bushy plants up to ~70 cm in diameter—approximately twice the size of typical perennial ryegrass under field conditions (Figure 1E,F). To our knowledge, this is the first report of such a mutation in *L. perenne*. The mutant has been named *VIROIZ*.

Figure 1. Phenotypic characteristics of the *VIROIZ* mutant of *L. perenne*. (**A**) Pot-grown mutant plant showing creeping stems; (**B**) single *VIROIZ* stem bearing four axillary shoots; (**C**) normal wild-type (WT) inflorescence; (**D**) variation in inflorescence morphology of *VIROIZ* plant showing reduced spikelet number and fasciation symptoms; (**E**) typical WT *L. perenne* plant; (**F**) clonally propagated *VIROIZ* plants grown in the field exhibiting a prostrate and bushy growth habit.

3.2. The Inheritance of the Spreading Growth Habit Evaluated in Field and Pot Experiments

The mutant was fertile and stable, and has been maintained through vegetative clonal propagation for several decades. To investigate the inheritance of the spreading growth habit, five pairwise crosses were made between the mutant and normal plants to produce F_1. In addition, F_2 populations were obtained from free-pollination of these five F_1 groups. S_1 of *VIROIZ* was also generated and evaluated in two separate experiments. Across all evaluations carried out in the field, the inheritance pattern of the spreading growth habit was similar: strictly mutant plants comprised 42–44% of each population, whereas plants with the wild-type habit comprised 8–14% (Figure 2). A considerable proportion of plants displayed intermediate phenotypes, ranging from 42–50%. Therefore, the deviation from the classical Mendelian 1:2:1 ratio for codominant trait segregation was evident, as confirmed by the χ^2 test ($p < 0.0001$; Table S1).

Additionally, in a pot experiment, the evaluation of the *VIROIZ* branching stem phenotype for axillary tiller development in two rounds of selection (positive and negative) was carried out, which revealed a clear pattern of trait divergence (Figure 3A–C). A selection at 10% intensity (34 of 340 genotypes) resulted in selected subpopulations C_0^+ and C_0^- with an average number of 3.41 and 1.83 axillary tillers per stem in the plant, respectively (Figure 3D). The second round of selection was performed with the same intensity as during the first cycle (10%, 34 selected genotypes), and it resulted in two subpopulations, C_1^+ and C_1^-. The average number of axillary tillers per stem in the plant was 3.90 and 0.22 in C_1^+ and C_1^-, respectively (Figure 3D). Thus, the selection differential was higher for negative selection (D = −1.76) than for positive selection (D = 1.44).

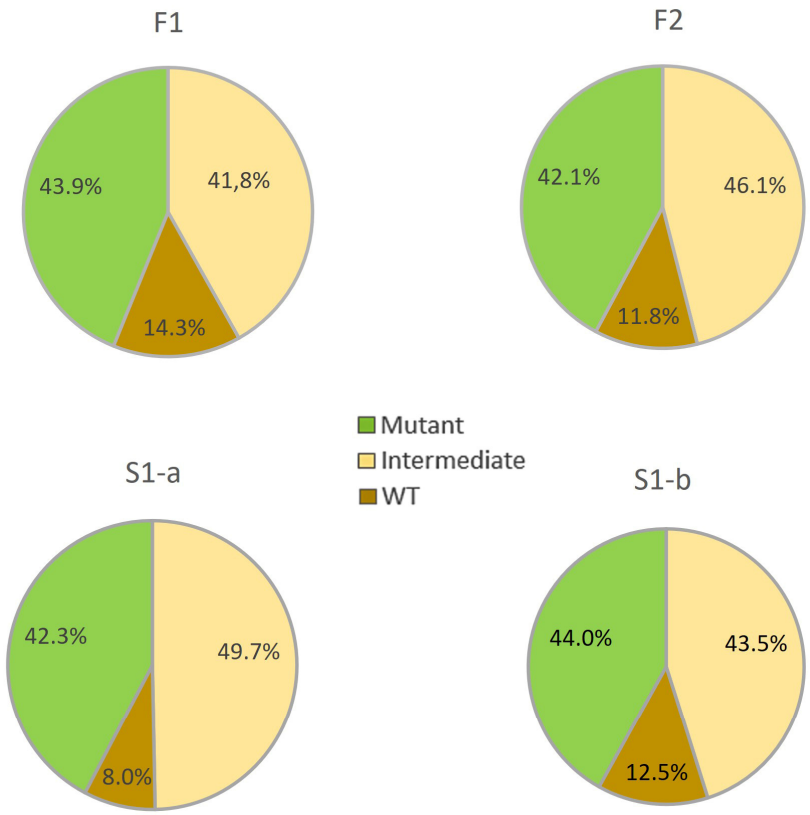

Figure 2. Distribution of the phenotypic spreading growth trait across generations. Mutant, wild-type (WT), and intermediate phenotypes were evaluated in single-plant field assessments: F1 (n = 285), F2 (n = 380), S1_a (n = 113), and S1_b (n = 142). Proportions of the mutant, WT, and intermediate plants have been consistent across generations. Chi-square test (χ^2 = 4.31, df = 6, p = 0.635).

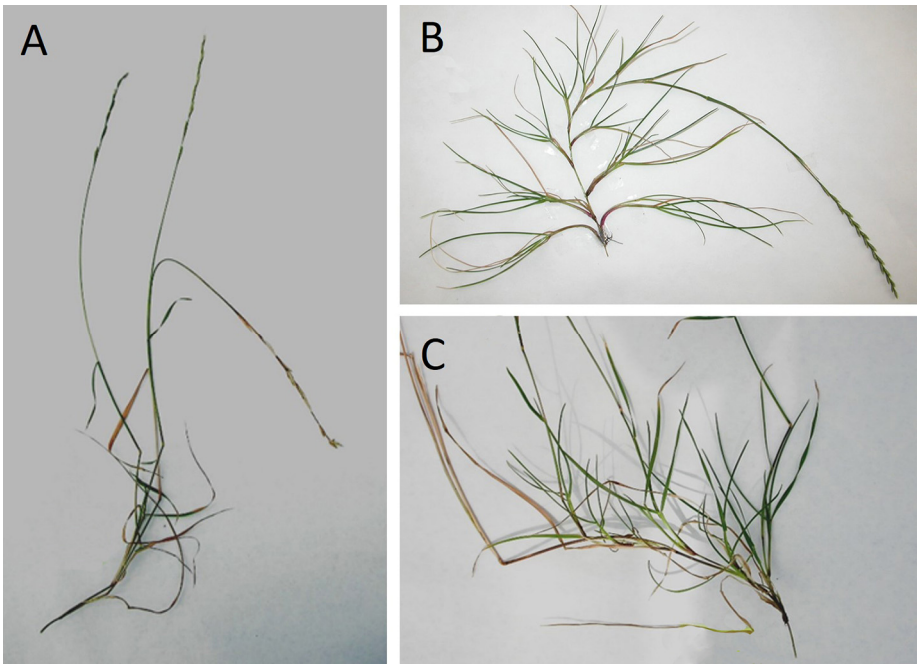

Figure 3. *Cont.*

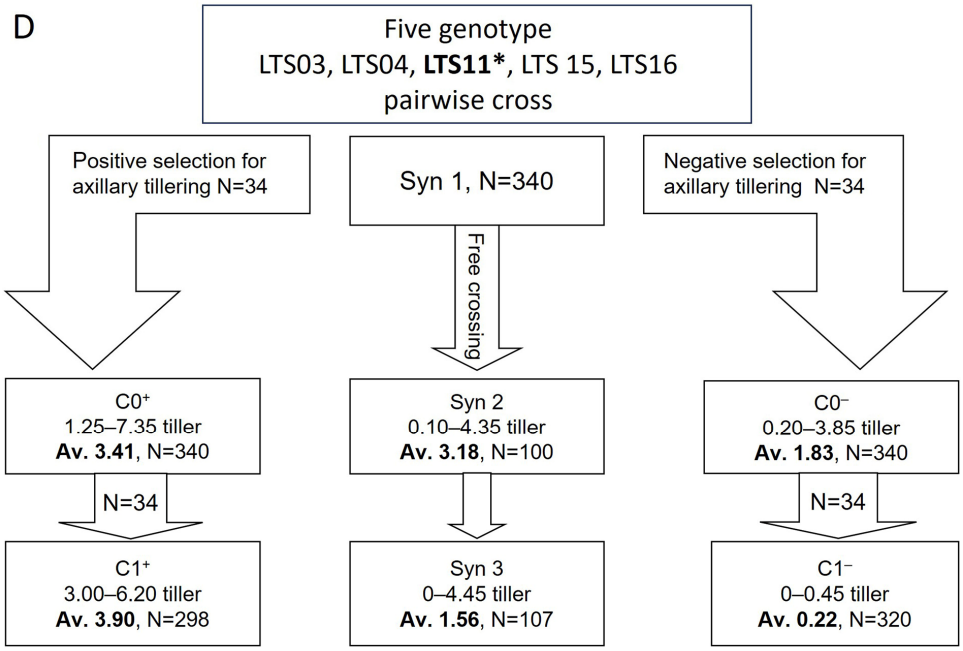

Figure 3. Patterns of divergent selection for the branching shoot trait resulting from axillary shoot development. (**A**) Typical wild-type (WT) shoot with no axillary tillers; (**B**,**C**) branching-type shoots with more than five axillary tillers; (**D**) schematic representation of divergent selection showing the change in the average number of axillary tillers per stem in the plant after two rounds of positive and negative selection. In both C^+ and C^- groups, the distribution of tiller numbers changed significantly from generation C_0 to C_1 (Chi-square test, p-value < 0.0001). Genotypes: LTS03 and LTS04 [30]; LTS11*—*VIROZ*; LTS 15 and LTS16 [29]. Av.—mean value for the group; N—number of plants.

3.3. Mutation Analysis of Candidate Genes Implicated in Shoot Morphogenesis

Partial sequencing of 11 candidate genes associated with shoot architecture was carried out, covering 40–90% of their full-length DNA coverage, aiming to explore the genetic basis of the altered stem-growth habit in *VIRIOZ*. The candidate genes were selected on the basis of their known roles in stem morphogenesis and the broad regulatory functions of the proteins they encode. These genes fall into the following functional groups: (i) classical hormone pathway regulators (*IAA1*, *BRI1*); (ii) strigolactone-related genes controlling shoot branching (*D27*, *CCD8*, *MAX2*); (iii) the *CRT3* gene encoding an ER chaperone interacting with BR signaling; (iv) proteasome- and ubiquitin-related genes (*UBC4*, *UBC10*, *RHF2A*, *RPT2A*); and (v) the protein kinase *CIPK9*, implicated in signaling pathways that influence shoot patterning. Three genes, *D27*, *UBC4*, and *CIPK9*, were sequenced to 80–90% of their full-length genomic DNA, four others, *IAA1I*, *BRI1*, *CRT3*, *MAX2*, between 50–70%, and the rest at ~40% of their length (Table 1). DNA sequences of these candidate genes from the *VIROIZ* mutant were aligned with those of wild-type (WT) plants (N = 6–17 individuals) and analysed using bioinformatic methods. Two mutant phenotype plants (SM117 and SM120) and two WT phenotype individuals (SW44 and SW84) from S1 selfing progeny were also included in the analysis (Figure S2). Partial sequencing of these genes did not provide a conclusive explanation for the altered stem-growth habit (Table 1). However, the most notable variation was detected in the *CRT3* gene: a point mutation c.1277C>G in exon 3 (corresponding to c.342C>G in cDNA from RNA transcript), leading to an amino acid substitution (p.L427V) (Table 1, Figure 4A,B). This mutation consistently distinguished the *VIROIZ* mutant and its mutant phenotype progeny in S1 from the WT group. Several indels were recorded in *CRT3* and *D27* of *VIROIZ*, though they were not unique to *VIROIZ* (Table 1, Figure 4C). Additional sequence alignments for the loci of the *D27*, *CCD8*, *MAX2*,

UBC4, *RHF2A*, and *CIPK9* genes are shown in Figure S3. From the partial sequencing data of these genes, no unique variants were found in *VIROIZ* compared with WT.

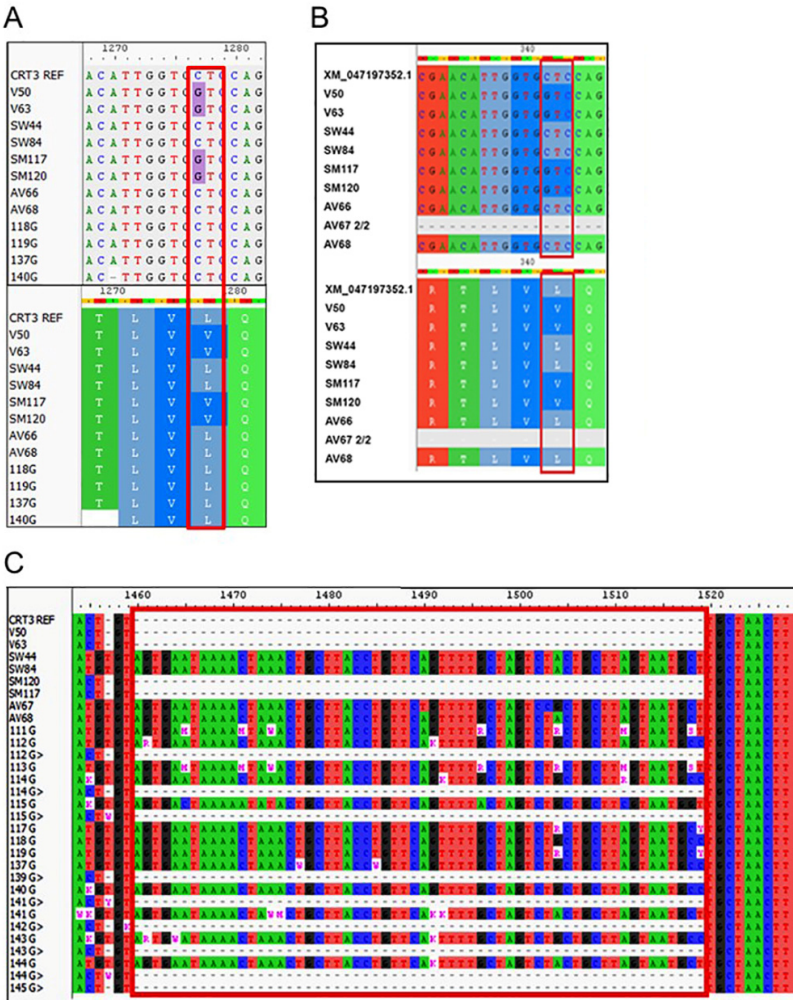

Figure 4. Comparison of *CRT3* sequences in *L. perenne* mutant and wild-type individuals. (**A**,**B**) Exon 3 and (**C**) intron 3 alignments. Red rectangles indicate sequence variants: in (**A**), the *VIROIZ*-specific substitution c.1277C>G (p.L427V); in (**B**) *CRT3* cDNA from RNA transcript confirms a unique variant in *VIROIZ* and mutant-type SM117 and SM120—c.342C>G, resulting in p.L427V (corresponding to c.1277C>G in (**A**); in (**C**), a 60 bp 1378_1440 indel is present across different genotypes. *CRT3* REF—*L. perenne* reference sequence. Note: V50, V63—*VIROIZ* mutant; SW44, SW84—WT type plants from *VIROIZ* self-pollination; SM117, SM120—mutant type from self-pollination. For comparison, WT genotypes from *L. perenne* 'Veja' (AV66, AV68, 115G, 117G, etc.) are included.

Table 1. Summary of candidate gene (partial sequence) screening for potential involvement in *VIROIZ* shoot morphology changes.

Gene	Protein Function	Full-Length Genomic DNA, bp	Gene Coverage in *VIROIZ*, bp (%)	Indel Allelic Variants		SNP Allelic Variants	
				Description	Status in *VIROIZ*	No.	Unique in *VIROIZ*
IAA1	Auxin-inducible transcriptional repressor	2552	1821 (71.4)	-	-	7	N*
BRI1	Receptor in brassinosteroids signaling	3837	1931 (50.3)	-	-	6	N

Table 1. *Cont.*

Gene	Protein Function	Full-Length Genomic DNA, bp	Gene Coverage in *VIROIZ*, bp (%)	Indel Allelic Variants		SNP Allelic Variants	
				Description	Status in *VIROIZ*	No.	Unique in *VIROIZ*
CRT3	ER chaperon for folding of BR receptors	4396	2584 (58.8)	1378_1440 indel, in3	Homozygote 62 bp (−/−) deletion	7	c.1277C>G (p.L427V)
D27 †	Strigolactone biosynthesis	2374	2138 (90.0)	g.463_467, in2; g.878_884, in3	Homozygote 5 bp insertion (+/+); Homozygote 7 bp deletion (−/−)	5	N
CCD8 †		3752	1572 (41.9)	g.3054_3072 indel, in3	Homozygote for 19 bp deletion (−/−)	8	N
MAX2 †	F-box protein in strigolactone signaling	4684	2840 (60.6)	-	-	1	N
UBC4 †	Ubiquitin-conjugating enzyme (E2)	2670	2274 (85.2)	-	-	-	N
UBC10	Ubiquitin-conjugating enzyme (E2)	3174	1361 (42.9)	-	-	2	N
RHF2A †	RING-E3 ubiquitin ligase	3408	1457 (42.8)	-	-	-	N
RPT2A	A 26S proteasome subunit	3104	1328 (42.8)	-	-	1	N
CIPK9 †	Protein kinase in signaling	4298	3905 (90.7)	-	-	-	N

Notes: N*—not unique; †—for these gene alignment views are shown in Figure S3.

3.4. Chromosome Pairing Irregularities in Meiosis

Meiosis was examined in the mutant and in F_1 hybrids obtained from crosses between the mutant and plants with the WT phenotype. In the mutant, meiosis proceeded regularly, with the formation of seven bivalents at metaphase I. In the F_1 hybrids, however, the chromosome pairing pattern in metaphase I was different. Two univalents (occasionally four) were consistently present, along with one of the bivalents appearing as a smaller, cross-shaped configuration distinct from the remaining five regular bivalents (Figure 5A–C). In tetrads, the presence of one or two micronuclei—likely originating from the univalents at earlier stages—was also observed (Figure 5D). These meiotic irregularities are indicative of chromosome translocations in *VIROIZ* and may contribute to its abnormal growth phenotype.

In summary, the *VIROIZ* mutant of *L. perenne* exhibits a unique spreading-growth habit characterized by prolific axillary shoot formation and prostrate and bushy growth. Field and pot evaluations confirmed the trait to be heritable, with populations consistently segregating into mutant, wild-type, and intermediate phenotypes, and the selection for axillary tiller number produced a clear divergence between selected positive and negative subpopulations. The partial sequencing of 11 candidate genes involved in hormone signaling, strigolactone-mediated branching, and proteasome function, all of which affect shoot patterning, revealed a notable point mutation in the *CRT3* gene c.1277C>G (p.L427V) (c.342C>G confirmed in cDNA from RNA transcript). This mutation was specific to the mutant and its mutant phenotype progeny and might have contributed to the enhanced branching and spreading stem phenotype. The cytological analysis indicated a largely normal meiosis in *VIROIZ*, but F_1 hybrids displayed univalents and micronuclei, suggesting underlying chromosome translocations present. Together, these results highlight *VIROIZ* as

a stable, heritable, and genetically distinct source of altered shoot architecture in perennial ryegrass.

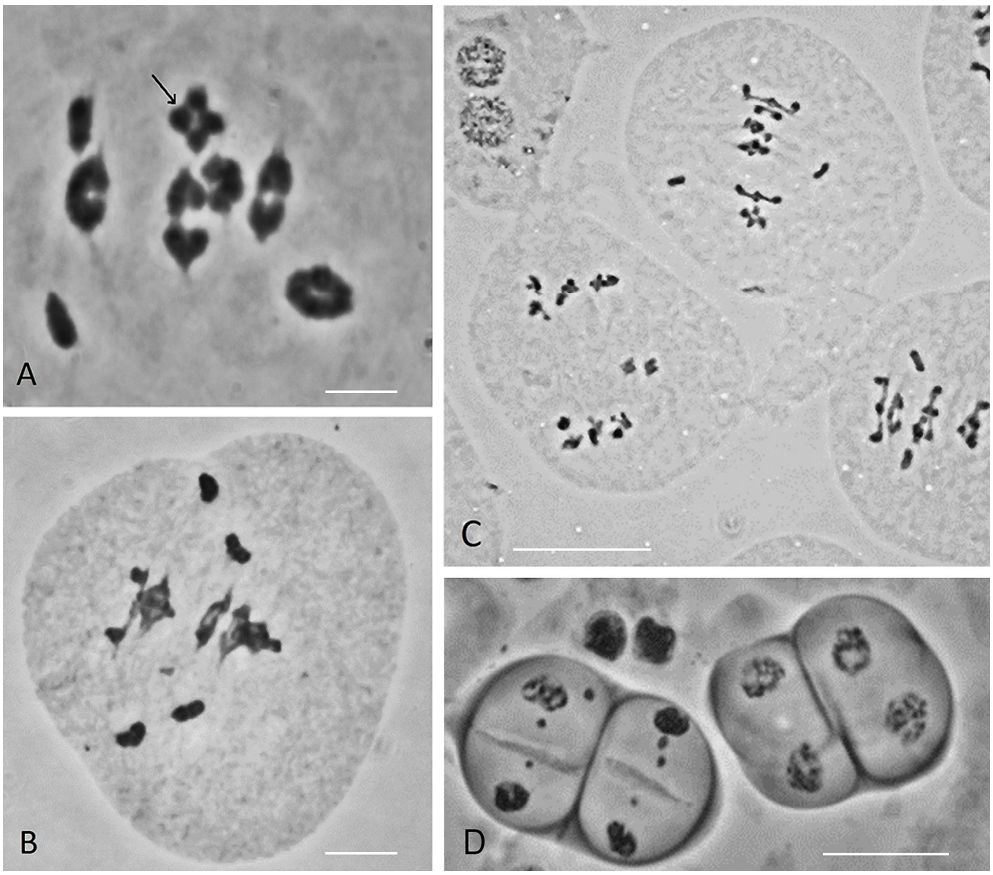

Figure 5. Meiotic metaphase I and tetrad stages in *VIROIZ* × WT F_1 hybrids. (**A**–**C**) Chromosome pairing patterns at metaphase I, showing a characteristic small cross-shaped bivalent (arrow in (**A**) together with two or four univalents not involved in pairing; (**D**) tetrads exhibiting micronuclei likely originating from univalents present at earlier stages. Scale bars: (**A**)—10 µm, (**B**)—20 µm, and (**C**,**D**)—40 µm.

4. Discussion

The *VIROIZ* mutant of *Lolium perenne* represents a novel and valuable genetic resource for exploring shoot architecture and turfgrass improvement. Morphologically, *VIROIZ* exhibits a distinctive spreading growth habit, characterized by prolific axillary shoot formation, prostrate and bushy growth. This growth habit results in dense plants nearly twice the size of the typical perennial ryegrass under field conditions, emphasizing the potential agronomic and aesthetic value of the mutation in turf applications. Reports of spreading or stoloniferous growth in *L. perenne* are rare, limited mainly to a patented *L. perenne* subsp. *stoloniferum* [15] and a few turf-type cultivars [9,16]. To our knowledge, *VIROIZ* represents the first well-documented, heritable mutation conferring a spreading growth habit in *L. perenne*, establishing it as a valuable breeding resource and model for dissecting the genetic regulation of shoot branching in perennial grasses.

The consistent expression of the *VIROIZ* spreading growth habit across F_1, F_2, and S_1 populations confirms its heritability and phenotypic stability. The segregation patterns suggest the involvement of one or more major loci, potentially modulated by additional factors. The presence of intermediate phenotypes is consistent with the quantitative and multifactorial nature of shoot branching, which is governed by hormonal signaling [18,23,34–36]. Furthermore, the observed responsiveness of *VIROIZ* to artificial selection, with distinct

divergent subpopulations, C_1^+ and C_1^-, emerging after only two selection cycles, underscores the plasticity of tiller number and suggests that this mutation could be exploited to fine-tune plant architecture in breeding programs, optimizing traits such as ground coverage and sward density for turf applications.

The partial sequencing of 11 candidate genes associated with shoot architecture did not provide a conclusive explanation for the altered phenotype. However, a nonsynonymous substitution was identified in exon 3 of the *CRT3* gene and confirmed in the transcript (c.342C>G; p.L427V), which was unique to the *VIROIZ* mutant and its mutant phenotype progeny. *CRT3* encodes an endoplasmic reticulum (ER) chaperone that interacts with brassinosteroid (BR) signaling components, ensuring proper folding and maturation of BR receptors [37]. Since BRs regulate cell elongation, organogenesis, and meristem activity, the impaired *CRT3* function could reduce BR receptor maturation and alter crosstalk with strigolactone, cytokinin, and auxin pathways, thereby releasing axillary buds from apical dominance [27,28,38–40]. In both *Arabidopsis* and rice, *CRT3* is co-expressed with genes involved in pathogen response and signal transduction [37,41]. Tissue-specific *CRT* expression, as seen in *Solanum lycopersicum*, suggests additional regulatory roles during development [42]. Beyond its functions in calcium storage and protein folding, CRT has been associated with the structure of plasmodesmata [43]. By facilitating the cell-to-cell transport of signaling molecules, including hormones, plasmodesmata may link CRTs to developmental regulatory pathways. While the *CRT3* mutation represents a promising candidate contributing to the *VIROIZ* phenotype, functional validation is required to confirm its causality. Nonetheless, other gene loci or structural variants cannot be ruled out, given the limitations of our partial sequencing data; therefore, future QTL mapping and genome-wide analyses will be needed to identify additional loci contributing to this trait.

In this study, we also examined canonical regulators of shoot branching. Among these, strigolactones are well-established repressors of axillary bud outgrowth across several plant species, acting in concert with auxin and BR signaling. Strigolactone synthesis and signaling mutants exhibit increased branching across multiple species—including *Arabidopsis*, pea, rice, petunia, and tomato [22,44–46]—and notably, the *VIROIZ* phenotype closely resembles the "branching stem" mutants observed in these model plants. In addition, many phytohormone signaling pathways rely on ubiquitin–proteasome–mediated degradation of repressors or inducers. Several of our selected candidate genes fall into these functional categories. However, partial sequencing of strigolactone-related genes (*D27*, *CCD8*, *MAX2*) and ubiquitin/proteasome-related genes (*UBC4*, *UBC10*, *RHF2A*, *RPT2A*) revealed no variants specific to *VIROIZ*. Future studies should therefore extend to full-length gene sequencing, transcriptomic profiling, and functional assays, since regulatory changes or post-translational modifications could also underlie the phenotype.

The cytological analysis has confirmed that *VIROIZ* maintains the diploid chromosome number ($2n = 2x = 14$) and undergoes normal meiosis. In contrast, F_1 hybrids between *VIROIZ* and wild-type plants exhibited meiotic irregularities, such as univalents, cross-shaped bivalents, and micronuclei, indicative of structural rearrangements, possibly translocations. The data supporting gross chromosomal rearrangements triggered by mutagenesis come from other species, for example, *Populus* [47]. The absence of abnormalities in the mutant, but their appearance in hybrids suggests heterozygosity for such rearrangements or compensatory mechanisms that stabilize meiosis in the mutant background. Structural changes of this kind can generate position effects on gene expression, raising the possibility that the *VIROIZ* phenotype reflects an interaction between chromosomal rearrangements and point mutation(s) such as that in *CRT3*. Whole-genome sequencing and functional assays will be critical to test this hypothesis.

5. Conclusions

The *VIROIZ* mutant represents the first documented heritable mutation conferring such a growth habit in *Lolium perenne*, making it suitable for breeding programs aimed at customizing canopy architecture for lawns and sports fields. From an applied perspective, the spreading, bushy growth of *VIROIZ* offers a substantial potential for turfgrass improvement, enhancing ground coverage and sward density. At the same time, potential trade-offs, such as effects on seed production and long-term persistence, should be evaluated in long-term field trials. In this study, molecular and cytological analyses implicate both a candidate point mutation in *CRT3* and possible chromosomal rearrangements affecting the altered phenotype; however, given the limitations of our partial sequencing data, other candidate genes cannot be ruled out in future studies. Together, these findings establish *VIROIZ* as both a practical breeding resource and a model for investigating the genetic control of shoot architecture in perennial grasses. Due to its perennial nature and stable growth habit, this mutant can be reliably maintained and shared for research and breeding purposes.

Supplementary Materials: The following supporting information can be downloaded at: https://www.mdpi.com/article/10.3390/agronomy15112541/s1, Figure S1: Field and Greenhouse Evaluations; Figure S2: Mutant type (SM120, SM117) and WT (SW84, SW44) plants from selfing; Figure S3: Gene loci alignment views in *VIROIZ* and WT; Table S1: Chi-square test for deviation from Mendelian ratio.

Funding: This study was partly funded by the EU Framework V project GRASP (QLRT-2001-0086).

Data Availability Statement: The original contributions presented in this study are included in the article/Supplementary Material. Further inquiries can be directed to the corresponding author.

Acknowledgments: The author gratefully acknowledges Gintaras Brazauskas for his contribution to the divergent selection experiment and Virginija Kvedienė for her technical assistance in plant evaluations. Appreciation is also extended to Domantas Palavenis and Vismantas Tučas for their contribution to gene screening.

Conflicts of Interest: The author declares no conflicts of interest.

References

1. Wilkins, P.W. Breeding Perennial Ryegrass for Agriculture. *Euphytica* **1991**, *52*, 201–214. [CrossRef]
2. Balfourier, F.; Charmet, G.; Ravel, C. Genetic Differentiation within and between Natural Populations of Perennial and Annual Ryegrass (*Lolium perenne* and *L. rigidum*). *Heredity* **1998**, *81*, 100–110. [CrossRef]
3. Wilkins, P.W.; Humphreys, M.O. Progress in Breeding Perennial Forage Grasses for Temperate Agriculture. *J. Agric. Sci.* **2003**, *140*, 129–150. [CrossRef]
4. Cui, Y.; Wang, J.; Wang, X.; Jiang, Y. Phenotypic and Genotypic Diversity for Drought Tolerance among and within Perennial Ryegrass Accessions. *HortScience* **2015**, *50*, 1148–1154. [CrossRef]
5. Grinberg, N.F.; Lovatt, A.; Hegarty, M.; Lovatt, A.; Skøt, K.P.; Kelly, R.; Blackmore, T.; Thorogood, D.; King, R.D.; Armstead, I.; et al. Implementation of Genomic Prediction in *Lolium perenne* (L.) Breeding Populations. *Front. Plant Sci.* **2016**, *7*, 133. [CrossRef]
6. Jaškūnė, K.; Aleliūnas, A.; Statkevičiūtė, G.; Kemešytė, V.; Studer, B.; Yates, S. Genome-Wide Association Study to Identify Candidate Loci for Biomass Formation under Water Deficit in Perennial Ryegrass. *Front. Plant Sci.* **2020**, *11*, 570204. [CrossRef] [PubMed]
7. Toporan, S.; Samfira, I. Review on the Genetic and Biochemical Characterization of *Lolium perenne* Species. *Res. J. Agric. Sci.* **2021**, *53*, 169–175.
8. Sampoux, J.P.; Baudouin, P.; Bayle, B.; Beguier, V.; Bourdon, P.; Chosson, J.F.; de Bruijn, K.; Deneufbourg, F.; Galbrun, C.; Ghesquière, M.; et al. Breeding Perennial Ryegrass (*Lolium perenne* L.) for Turf Usage: An Assessment of Genetic Improvements in Cultivars Released in Europe, 1974–2004. *Grass Forage Sci.* **2012**, *68*, 33–48. [CrossRef]
9. Pornaro, C.; Menegon, A.; Macolino, S. Stolon Development in Four Turf-Type Perennial Ryegrass Cultivars. *Agron. J.* **2018**, *110*, 2159–2164. [CrossRef]
10. Terrell, E.E. *A Taxonomic Revision of the Genus Lolium*, Technical Bulletin; United States Department of Agriculture, Economic Research Service: Washington, DC, USA, 1968; No. 171644.

11. Langer, R.H.M. *How Grasses Grow*; Edward Arnold Publishers Limited: London, UK, 1979.
12. Kydd, D.D. The Effect of Intensive Sheep Stocking over a Five-Year Period on the Development and Production of the Sward. *J. Br. Grassl. Soc.* **1966**, *21*, 284–288. [CrossRef]
13. Hayes, P. Stoloniferous Perennial Ryegrass (*Lolium perenne*) in Northern Ireland Paddocks. *Rec. Agric. Res. Minist. Agric. N. Irel.* **1971**, *19*, 63–64.
14. Harris, W.; Pandey, K.K.; Gray, Y.S.; Couchman, P.K. Observations on the Spread of Perennial Ryegrass by Stolons in a Lawn. *N. Z. J. Agric. Res.* **1979**, *22*, 61–68. [CrossRef]
15. Wipff, J.K.; Singh, D. Lolium perenne subsp. Stoloniferum; Perennial Ryegrass with Determinate Stolons. U.S. Plant Patent No. US8927804B2, 6 January 2015.
16. Masin, R.; Macolino, S. Seedling Emergence and Establishment of Annual Bluegrass (*Poa annua*) in Turfgrasses of Traditional and Creeping Perennial Ryegrass Cultivars. *Weed Technol.* **2016**, *30*, 238–245. [CrossRef]
17. Dun, E.A.; Brewer, P.B.; Beveridge, C.A. Strigolactones: Discovery of the Elusive Shoot Branching Hormone. *Trends Plant Sci.* **2009**, *14*, 364–372. [CrossRef] [PubMed]
18. Domagalska, M.A.; Leyser, O. Signal Integration in the Control of Shoot Branching. *Nat. Rev. Mol. Cell Biol.* **2011**, *12*, 211–221. Available online: https://www.nature.com/articles/nrm3088 (accessed on 15 October 2025). [CrossRef]
19. Dun, E.A.; de Saint Germain, A.; Rameau, C.; Beveridge, C.A. Dynamics of Strigolactone Function and Shoot Branching Responses in *Pisum sativum*. *Mol. Plant* **2013**, *6*, 128–141. [CrossRef] [PubMed]
20. Dun, E.A.; Brewer, P.B.; Gillam, E.M.J.; Beveridge, C.A. Strigolactones and Shoot Branching: What Is the Real Hormone and How Does It Work? *Plant Cell Physiol.* **2023**, *64*, 967–983. [CrossRef]
21. Ongaro, V.; Leyser, O. Hormonal Control of Shoot Branching. *J. Exp. Bot.* **2008**, *59*, 67–74. [CrossRef]
22. Beveridge, C.A.; Dun, E.A.; Rameau, C. Pea Has Its Tendrils in Branching Discoveries Spanning a Century from Auxin to Strigolactones. *Plant Physiol.* **2009**, *151*, 985–990. [CrossRef]
23. Zhang, N.; Liu, Y.; Gui, S.; Wang, Y. Regulation of Tillering and Panicle Branching in Rice and Wheat. *J. Genet. Genom.* **2025**, *52*, 869–886. [CrossRef]
24. Pašakinskienė, I. Creeping Stem and Barren Inflorescence: A New Mutation in *Lolium perenne* "VIROIZ". In *Recent Advances in Genetics and Breeding of the Grasses*; Institute of Plant Genetics: Poznan, Poland, 2005; pp. 209–213.
25. Francis, A.; Jones, R.N. Heritable Nature of Colchicine-Induced Variation in Diploid *Lolium perenne*. *Heredity* **1989**, *62*, 407–410. [CrossRef]
26. Brazauskas, G.; Pašakinskienė, I.; Asp, T.; Lübberstedt, T. Nucleotide Diversity and Linkage Disequilibrium in Five *Lolium perenne* Genes with Putative Role in Shoot Morphology. *Plant Sci.* **2010**, *179*, 194–201. [CrossRef]
27. Clouse, S.D. Brassinosteroid Signal Transduction: From Receptor Kinase Activation to Transcriptional Networks Regulating Plant Development. *Plant Cell* **2011**, *23*, 1219–1230. [CrossRef] [PubMed]
28. Tong, H.; Chu, C. Functional Specificities of Brassinosteroid and Potential Utilization for Crop Improvement. *Trends Plant Sci.* **2018**, *23*, 1016–1028. [CrossRef] [PubMed]
29. Murashige, T.; Skoog, F. A Revised Medium for Rapid Growth and Bioassays with Tobacco Tissue Cultures. *Physiol. Plant.* **1962**, *15*, 473–497. [CrossRef]
30. Pašakinskienė, I. Culture of Embryos and Shoot Tips for Chromosome Doubling in *Lolium perenne* and Sterile Hybrids between *Lolium* and *Festuca*. *Plant Breed.* **2000**, *119*, 185–187. [CrossRef]
31. Posselt, U.K.; Barre, P.; Brazauskas, G.; Turner, L.B. Comparative Analysis of Genetic Similarity between Perennial Ryegrass Genotypes Investigated with AFLPs, SSRs, RAPDs, and ISSRs. *Czech J. Genet. Plant Breed.* **2006**, *42*, 87–94. [CrossRef]
32. Jensen, L.B.; Andersen, J.R.; Frei, U.; Xing, Y.; Taylor, C.; Holm, P.B.; Lübberstedt, T. QTL Mapping of Vernalization Response in Perennial Ryegrass (*Lolium perenne* L.) Reveals Co-Location with an Orthologue of Wheat *VRN1*. *Theor. Appl. Genet.* **2005**, *110*, 527–536. [CrossRef]
33. Larsson, A. AliView: A Fast and Lightweight Alignment Viewer and Editor for Large Datasets. *Bioinformatics* **2014**, *30*, 3276–3278. [CrossRef]
34. Wang, Y.; Wang, J.; Shi, B.; Yu, T.; Qi, J.; Meyerowitz, E.M.; Jiao, Y. The Stem Cell Niche in Leaf Axils Is Established by Auxin and Cytokinin in *Arabidopsis*. *Plant Cell* **2018**, *26*, 2055–2067. [CrossRef]
35. Tavares, H.; Readshaw, A.; Kania, U.; de Jong, M.; Pasam, R.K.; McCulloch, H.; Ward, S.; Shenhav, L.; Forsyth, E.; Leyser, O. Artificial Selection Reveals Complex Genetic Architecture of Shoot Branching and Its Response to Nitrate Supply in *Arabidopsis*. *PLoS Genet.* **2023**, *19*, e1010863. [CrossRef] [PubMed]
36. Yuan, Y.; Khourchi, S.; Li, S.; Du, Y.; Delaplace, P. Unlocking the Multifaceted Mechanisms of Bud Outgrowth: Advances in Understanding Shoot Branching. *Plants* **2023**, *12*, 3628. [CrossRef] [PubMed]
37. Jin, H.; Hong, Z.; Su, W.; Li, J. A Plant-Specific Calreticulin Is a Key Retention Factor for a Defective Brassinosteroid Receptor in the Endoplasmic Reticulum. *Proc. Natl. Acad. Sci. USA* **2009**, *106*, 13612–13617. [CrossRef] [PubMed]
38. Li, Z.; He, Y. Roles of Brassinosteroids in Plant Reproduction. *Int. J. Mol. Sci.* **2020**, *21*, 872. [CrossRef]

39. Mao, J.; Li, J. Regulation of Three Key Kinases of Brassinosteroid Signaling Pathway. *Int. J. Mol. Sci.* **2020**, *21*, 4340. [CrossRef]
40. Xia, X.; Dong, H.; Yin, Y.; Song, X.; Gu, X.; Sang, K.; Zhou, J.; Shi, K.; Zhou, Y.; Foyer, C.H.; et al. Brassinosteroid Signaling Integrates Multiple Pathways to Release Apical Dominance in Tomato. *Proc. Natl. Acad. Sci. USA* **2021**, *118*, e2004384118. [CrossRef]
41. Thelin, L.; Mutwil, M.; Sommarin, M.; Persson, S. Diverging Functions among Calreticulin Isoforms in Higher Plants. *Plant Signal. Behav.* **2011**, *6*, 905–910. [CrossRef]
42. Muhammad, T.; Yang, T.; Wang, B.; Yang, H.; Tuerdiyusufu, D.; Wang, J.; Yu, Q. Comprehensive Genomic Characterization and Expression Analysis of Calreticulin Gene Family in Tomato. *Front. Plant Sci.* **2024**, *15*, 1397765. [CrossRef]
43. Baluška, F.; Šamaj, J.; Napier, R.; Volkmann, D. Maize Calreticulin Localizes Preferentially to Plasmodesmata in Root Apex. *Plant J.* **1999**, *19*, 481–488. [CrossRef]
44. Leyser, O. The Control of Shoot Branching: An Example of Plant Information Processing. *Plant Cell Environ.* **2009**, *32*, 694–703. [CrossRef]
45. Beveridge, C.A.; Kyozuka, J. New Genes in Strigolactone-Related Shoot Branching Pathway. *Curr. Opin. Plant Biol.* **2010**, *13*, 34–39. [CrossRef]
46. Wu, F.; Gao, Y.; Yang, W.; Sui, N.; Zhu, J. Biological Functions of Strigolactones and Their Crosstalk with Other Phytohormones. *Front. Plant Sci.* **2022**, *13*, 821563. [CrossRef]
47. Guo, W.; Comai, L.; Henry, I.M. Chromoanagenesis from Radiation-Induced Genome Damage in *Populus*. *PLoS Genet.* **2021**, *17*, e1009735. [CrossRef]